JACS
JOURNAL OF THE AMERICAN CHEMICAL SOCIETY
pubs.acs.org/JACS
Communication

# Templation and Concentration Drive Conversion Between a $Fe^{II}_{12}L_{12}$ Pseudoicosahedron, a $Fe^{II}_{4}L_{4}$ Tetrahedron, and a $Fe^{II}_{2}L_{3}$ Helicate

Dawei Zhang, Quan Gan, Alex J. Plajer, Roy Lavendomme, Tanya K. Ronson, Zifei Lu, Jesper D. Jensen, Bo W. Laursen, and Jonathan R. Nitschke*

Cite This: *J. Am. Chem. Soc.* 2022, 144, 1106–1112



**ABSTRACT:** We report the construction of three structurally distinct self-assembled architectures: $Fe^{II}_{12}L_{12}$ pseudoicosahedron **1**, $Fe^{II}_{2}L_{3}$ helicate **2**, and $Fe^{II}_{4}L_{4}$ tetrahedron **3**, formed from a single triazatriangulenium subcomponent **A** under different reaction conditions. Pseudoicosahedral capsule **1** is the largest formed through subcomponent self-assembly to date, with an outer-sphere diameter of 5.4 nm and a cavity volume of 15 $nm^3$. The outcome of self-assembly depended upon concentration, where the formation of pseudoicosahedron **1** was favored at higher concentrations, while helicate **2** exclusively formed at lower concentrations. The conversion of pseudoicosahedron **1** or helicate **2** into tetrahedron **3** occurred following the addition of a $CB_{11}H_{12}^-$ or $B_{12}F_{12}^{2-}$ template.

Coordination-driven self-assembly is an efficient tool for the construction of polyhedral metal−organic complexes,[1] the cavities of which have proven useful in a range of applications, including molecular recognition,[2] stereochemical sensing,[3] chemical separation,[4] stabilization of reactive species,[5] and catalysis.[6] The strategy of subcomponent self-assembly,[7] involving the formation of structures containing multiple N→metal and C═N linkages during the same overall process, allows the preparation of a variety of capsules with different shapes and cavity sizes, which bind many different guests.[7a]

An attractive goal is the construction of large self-assembled architectures[8] that resemble the icosahedral structures adopted by some protein cages.[9] As in the cases of icosahedral viral capsids assembled from multiple copies of a single protein subunit, self-assembly can allow the construction of larger architectures from much smaller components. The large internal voids of capsules with a sufficient degree of cavity enclosure may be suitable for binding large substrates,[10] enabling synthetic encapsulants to approach the complex functions exhibited by biological systems.

In analogy to the structural changes of biological molecules,[11] designing stimuli-responsive transformations within systems of discrete self-assembled container molecules is an important challenge in supramolecular chemistry.[12] Such transformations may lead to functions that include guest uptake and release,[13] chemical purification,[14] reagent storage,[15] and drug delivery.[16] Various stimuli, such as light,[13b,17] pH,[18] temperature,[19] solvent,[2c,20] concentration,[21] or additional chemical signals,[22] have been employed to trigger transformation processes that lead to structural conversions. Supramolecular transformations involving multiple different structure types based upon a single ligand and metal ion remain rare,[23] however.

Here, we report the preparation of three different architectures, a $Fe^{II}_{12}L_{12}$ pseudoicosahedron, a $Fe^{II}_{2}L_{3}$ helicate, and a $Fe^{II}_{4}L_{4}$ tetrahedron, assembled from the same triazatriangulenium (TATA) subcomponent under different reaction conditions. Changes in ligand concentration or the addition of template anions triggered complete conversions between these assemblies.

Subcomponent **A** (Figure 1) was prepared following our previously reported procedure.[24] We first explored its self-assembly at a concentration of 4.4 mM in acetonitrile. The reaction of subcomponents **A** (1 equiv) and *p*-anisidine (3 equiv) with $Fe(BF_4)_2$ (1 equiv) in acetonitrile at 70 °C resulted in the formation of the very large architecture **1**. ESI-MS showed a series of sharp peaks (Figure 2b), corresponding to charge states from 18+ to 11+, all of which were consistent with a $Fe^{II}_{12}L_{12}$ composition.

The $^1$H NMR spectrum of $Fe^{II}_{12}L_{12}$ **1** displayed a complex pattern of signals, consistent with desymmetrization of the ligand (Figures 2a and S4). Three magnetically distinct chemical environments for the protons on the initially $C_3$-symmetric ligand were observed, with the imine and methoxy signals each exhibiting three sharp peaks with a 1:1:1 integration ratio. The $^1$H DOSY spectrum confirmed that all $^1$H signals belonged to a single species in solution (Figures 2a and S10).

These NMR and MS data were consistent with the formation of a $Fe^{II}_{12}L_{12}$ pseudoicosahedral capsule with *meridional* (*mer*) coordination geometry at all iron(II) vertices (Figure 1a). The $^1$H NMR spectrum of **1** was fully assigned through 2D NMR (Figures S7−S9). This type of assembly has

**Received:** November 1, 2021
**Published:** January 11, 2022

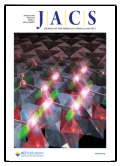





https://doi.org/10.1021/jacs.1c11536
*J. Am. Chem. Soc.* 2022, 144, 1106−1112

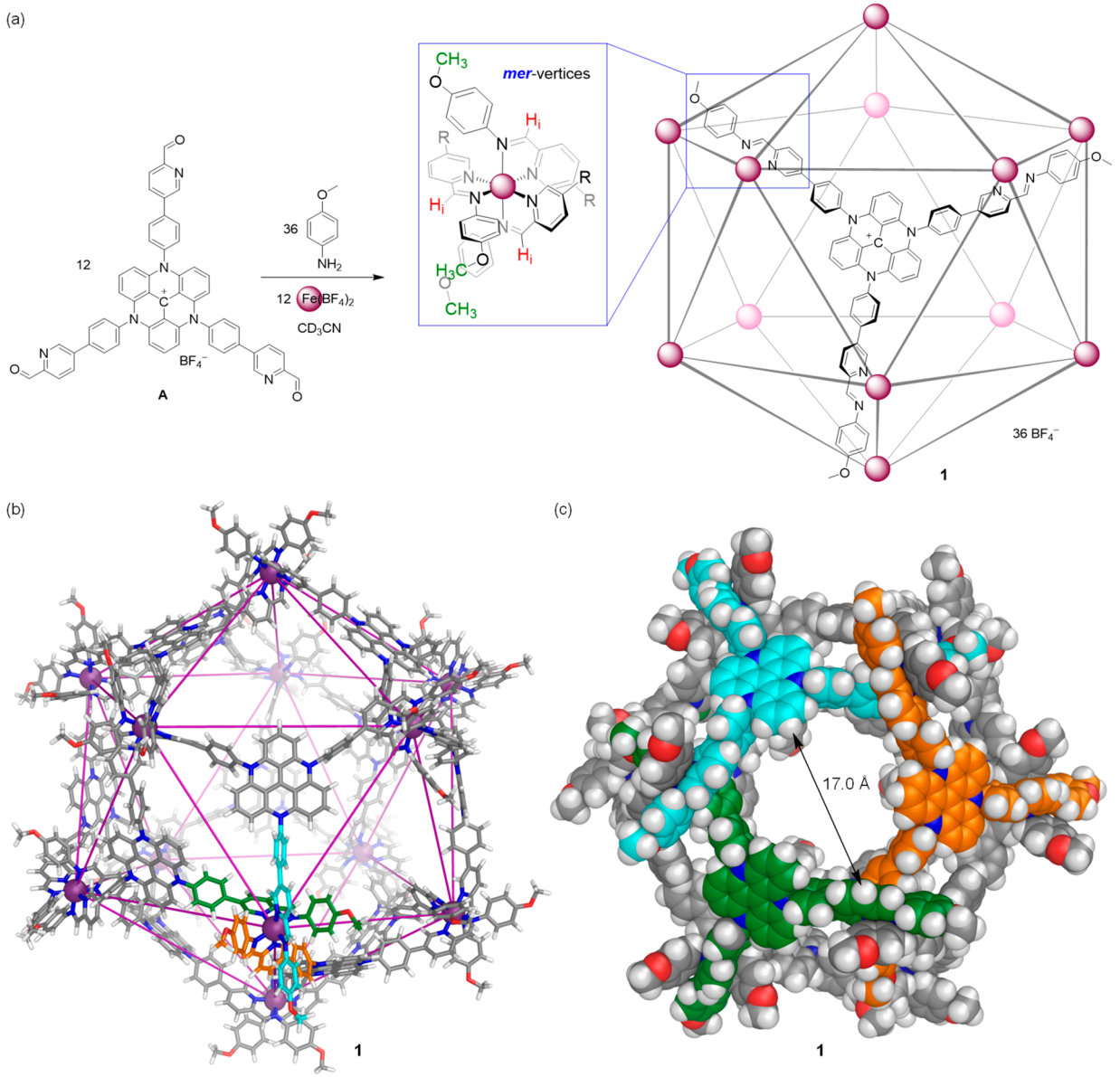


**Figure 1.** (a) Subcomponent self-assembly of $Fe^{II}_{12}L_{12}$ pseudoicosahedron **1**, with cutout showing the *meridional* metal coordination geometry. (b) PM7-optimized molecular model of pseudoicosahedron **1**. Carbon atoms for the three distinct ligand arms about one of the *mer*-vertices have been colored cyan, green, and orange, respectively. (c) Model of **1** in space-filling mode, to show the porosity. Carbon atoms of the three triazatriangulenium ligands surrounding a large pore of **1** have been colored cyan, green, and orange, respectively.

been observed for a smaller $C_3$-symmetric triamine subcomponent, where a mixture of pseudoicosahedron and tetrahedron was obtained.[25] We infer the formation of the larger capsule, rather than a $Fe^{II}_4L_4$ tetrahedral cage, to result from the Coulombic repulsions between the cationic triazatriangulenium panels, which would be stronger in a tetrahedron where these panels are spatially closer together.

After many unsuccessful attempts at growing crystals of **1** suitable for X-ray diffraction, energy minimization of a pseudoicosahedral structure for **1** at the PM7 level of theory was carried out (Figure 1b and Table S2). The 12 iron(II) centers describe the vertices of an icosahedron, with the tris(bidentate) ligands capping 12 of the 20 icosahedral faces. All iron(II) centers in **1** display *mer* coordination around the metal centers, where two ligand arms extend above a triangular face of the "icosahedron" (Figure 1b, cyan and orange) and the third extends from below (Figure 1b, green). The longest Fe···Fe distance between antipodal vertices within this model of **1** is 4.1 nm, and the longest distance between the outermost methoxy groups is approximately 5.4 nm.

The PM7 model also indicates the capsule to be porous, with $C_3$-symmetric openings, having diameters of as large as 17 Å, each surrounded by three TATA ligands (one type of opening is shown in Figure 1c). Pseudoicosahedron **1** encloses a cavity volume of 15095 $Å^3$, as determined by VOIDOO calculations (Table S1).[26] Capsule **1** thus represents the largest architecture prepared to date, to the best of our knowledge, using subcomponent self-assembly.[7i,25,27]

As the cavity of pseudoicosahedron **1** is large and positively charged, we tested the binding of a series of large anionic and neutral prospective guests. None of these prospective guests, listed in Scheme S3, gave any evidence of guest encapsulation. We infer that they are not large enough to provide a good fit



https://doi.org/10.1021/jacs.1c11536
J. Am. Chem. Soc. 2022, 144, 1106−1112

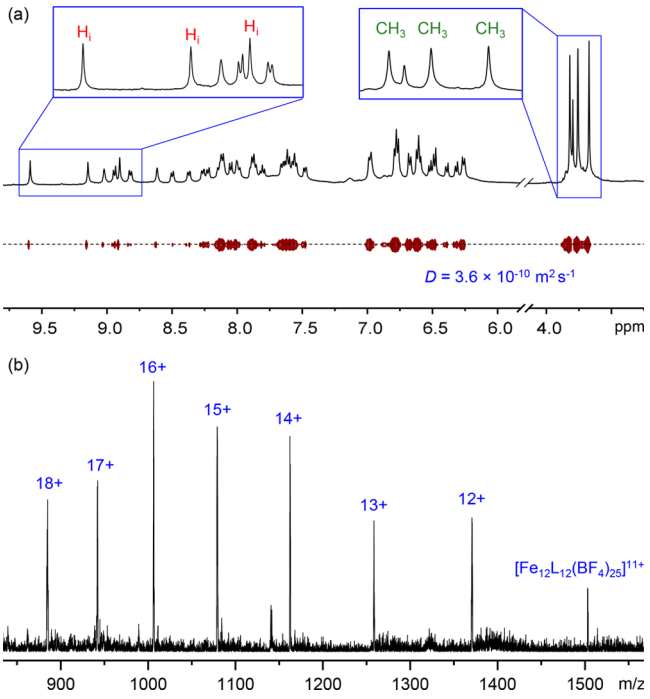


**Figure 2.** (a) $^1$H DOSY NMR spectrum (500 MHz, 298 K, $CD_3CN$) of pseudoicosahedron **1**. The labeled peaks correspond to the imine and methoxy groups are highlighted in Figure 1a. (b) ESI-mass spectrum of **1**.

for the cavity, as most have been reported to be encapsulated within smaller capsules.[28]

In contrast, when **A** (1 equiv) reacted with *p*-anisidine (3 equiv) and $Fe(BF_4)_2$ (either 0.67 or 1 equiv gave the same result) in acetonitrile at the lower **A** concentration of 2.2 mM, helicate **2** was formed instead of **1** (Scheme S4 and Figures S11–S16). An overall 7+ charge for **2** was confirmed by ESI-MS (Figure S17). The $^1$H NMR spectrum of **2** displayed signals corresponding to a $C_2$-symmetric bis-bidentate ligand, with one pyridyl-imine arm remaining uncoordinated (Figure S11). Both the imine and methoxy $^1$H NMR signals of **2** exhibited a 2:1 integral ratio, consistent with the formation of a helicate with $D_3$ symmetry, in which both iron(II) centers adopted the same Λ or Δ handedness.[22,29]

The formation of smaller assembly **2** at a lower concentration is expected on the basis of Le Chatelier's principle.[30] The electrostatic interactions between the small $BF_4^-$ anion and the small cavities of the cationic assembly may also render $BF_4^-$ a suitable template for helicate formation.

The anion binding ability of helicate **2** was confirmed by carrying out $^1$H NMR titrations. The progressive addition of tetrabutylammonium perchlorate to a solution of **2** in $CD_3CN$ resulted in displacement of $BF_4^-$ by $ClO_4^-$, as indicated by shifts in the helicate $^1$H signals, consistent with binding in fast exchange on the NMR chemical shift time scale (Figure S18). The addition of excess $ReO_4^-$, $PF_6^-$, or $I^-$ led to similar NMR observations, but $Tf_2N^-$ did not (Figure S19). The lack of shifts in the $^1$H signals of **2** (<0.02 ppm at most) after adding excess $Tf_2N^-$ indicated negligible interactions of this anion with helicate **2** relative to $BF_4^-$.

Although numerous attempts to obtain the crystal structure of a host–guest complex of **2** were unsuccessful, we were able to obtain the crystal structure of a host–guest complex of its structural analogue **2′**, which assembled from a similar subcomponent (**B**) bearing only two pyridine-aldehyde functionalities (Figures 3a and S20–S26). Helicate **2′** bound anions in solution in similar fashion to **2** (Figure S27).

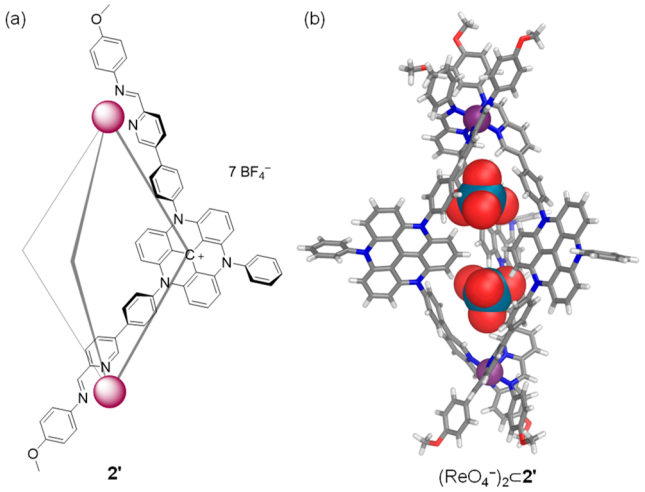


**Figure 3.** Schematic drawing of **2′** (a) and X-ray crystal structure of $(ReO_4^-)_2\subset$**2′** (b). Disorder, noncentrally bound counterions, and solvent of crystallization are omitted for clarity.

Slow vapor diffusion of diethyl ether into an acetonitrile solution of **2′** in the presence of $ReO_4^-$ yielded crystals of $(ReO_4^-)_2\subset$**2′** suitable for X-ray diffraction. Two $ReO_4^-$ anions were found within two distinct cavities of helicate **2′**, separated by the three converging TATA moieties (Figure 3b). Each of the two cavities is surrounded by three phenyl rings, giving cavity volumes of 76 and 77 Å$^3$ (Table S1). The two iron(II) centers of **2′**, separated by 20.0 Å, have the same handedness, generating a structure with $D_3$ symmetry, consistent with solution NMR spectra.

When larger anions were added to helicate **2** in solution, such as carba-*closo*-dodecaborate ($CB_{11}H_{12}^-$) or dodecafluoro-*closo*-dodecaborate ($B_{12}F_{12}^{2-}$), full conversion into tetrahedron **3** was observed after 12 h, resulting in a set of ligand $^1$H NMR signals consistent with a *T*-symmetric tetrahedral cage (Figures 4 and S28–S37). The $Fe^{II}_4L_4$ composition of **3** was confirmed by ESI-MS (Figures S30 and S35). These results suggested that $CB_{11}H_{12}^-$ and $B_{12}F_{12}^{2-}$ could serve as templates to bring four cationic ligands together into the tetrahedral framework of **3**, overcoming interligand Columbic repulsions.[31] A cavity volume of 371 Å$^3$ was calculated based on a PM7 model of **3** (Table S4), substantially smaller than that of pseudoicosahedron **1** (15095 Å$^3$) and larger than the twin cavities of **2** (55 Å$^3$ each when calculated from a PM7 model of **2** in the absence of bound anions, see Table S3) (Table S1). Conversion of pseudoicosahedron **1** into tetrahedron **3** also occurred following the addition of either of the template anions $CB_{11}H_{12}^-$ or $B_{12}F_{12}^{2-}$ (Figure 4).

In summary, we have demonstrated the construction of a series of distinct capsules under different reaction conditions from TATA-containing subcomponent **A**, from large pseudoicosahedron **1**, to medium-sized tetrahedron **3** and smaller helicate **2**. These structures have drastically different cavity volumes, shapes, and sizes. Pseudoicosahedron **1** encloses a cavity volume that may allow the encapsulation of guests with diameters in the range of 3–4 nm.[10] Prior studies of smaller TATA-based metal–organic assemblies have shown binding to


https://doi.org/10.1021/jacs.1c11536
J. Am. Chem. Soc. 2022, 144, 1106–1112

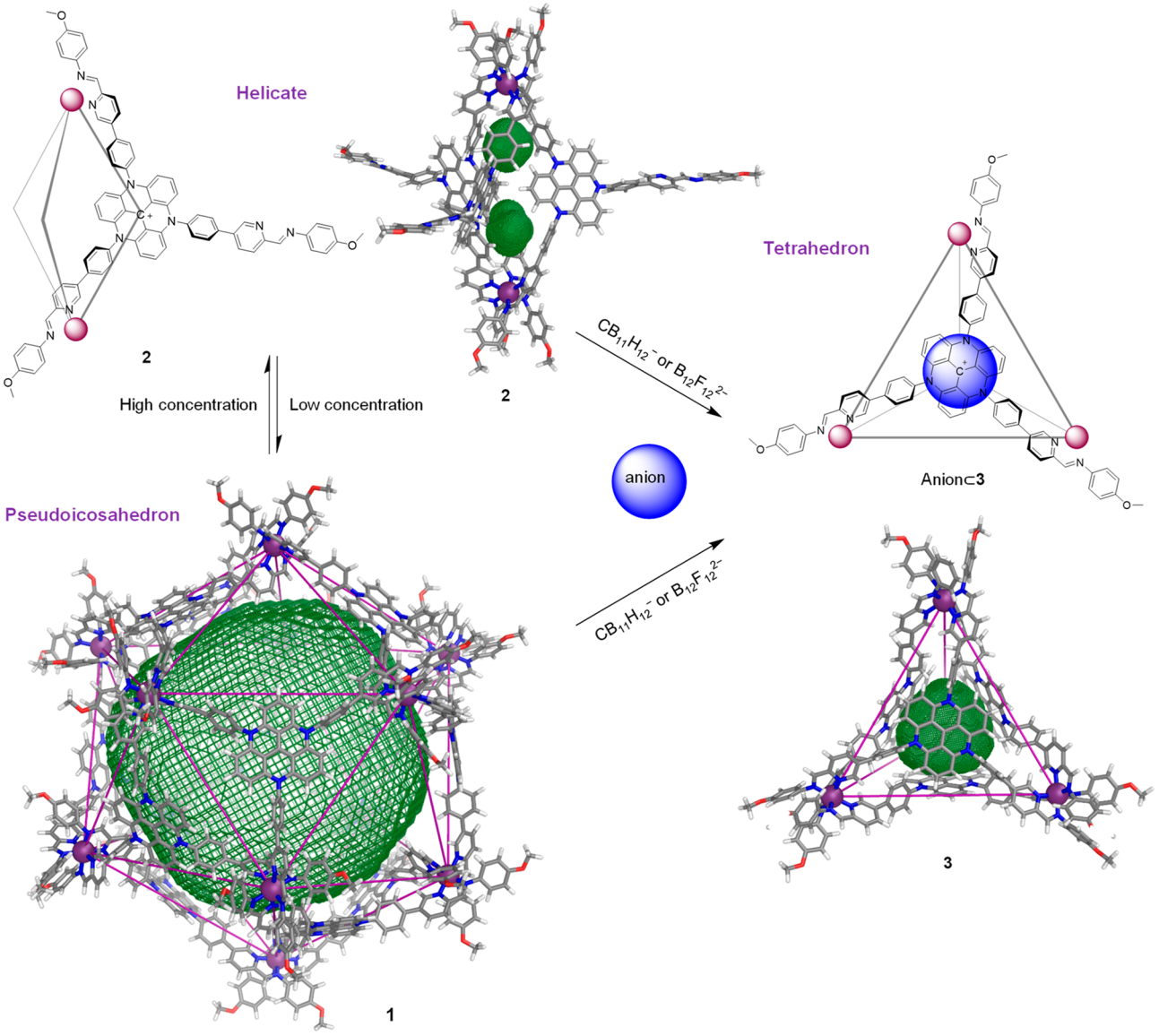


**Figure 4.** Interconversion between pseudoicosahedron **1**, helicate **2**, and tetrahedron **3**, showing PM7-optimized molecular models of each with the cavity volumes outlined in green mesh. Pseudoicosahedron **1** and helicate **2** interconverted following a change in ligand concentration. Addition of $CB_{11}H_{12}^-$ or $B_{12}F_{12}^{2-}$ to assembly **1** or **2** drove the formation of tetrahedron **3**, with the template anion bound inside the cavity.

small biological anions in water,[24] suggesting that water-soluble versions[32] of pseudoicosahedron **1** may prove useful for binding larger and more complex biomolecules, such as proteins and nucleic acids.

## ■ ASSOCIATED CONTENT

### Supporting Information

The Supporting Information is available free of charge at https://pubs.acs.org/doi/10.1021/jacs.1c11536.

Complete experimental details X-ray data for $(ReO_4^-)_2$⊂**2′** (CCDC 2071272) (PDF)

### Accession Codes

CCDC 2071272 contains the supplementary crystallographic data for this paper. These data can be obtained free of charge via www.ccdc.cam.ac.uk/data_request/cif, or by emailing data_request@ccdc.cam.ac.uk, or by contacting The Cambridge Crystallographic Data Centre, 12 Union Road, Cambridge CB2 1EZ, UK; fax: +44 1223 336033.

## ■ AUTHOR INFORMATION


### Corresponding Author

**Jonathan R. Nitschke** − *Department of Chemistry, University of Cambridge, Cambridge CB2 1EW, United Kingdom*; Email: jrn34@cam.ac.uk

### Authors

**Dawei Zhang** − *Shanghai Key Laboratory of Green Chemistry and Chemical Processes, School of Chemistry and Molecular Engineering, East China Normal University, Shanghai 200062, People's Republic of China; Department of Chemistry, University of Cambridge, Cambridge CB2 1EW, United Kingdom;* orcid.org/0000-0002-0898-9795

**Quan Gan** − *Department of Chemistry, University of Cambridge, Cambridge CB2 1EW, United Kingdom; Hubei Key Laboratory of Bioinorganic Chemistry & Materia Medica, School of Chemistry and Chemical Engineering, Huazhong University of Science and Technology, Wuhan*




https://doi.org/10.1021/jacs.1c11536
J. Am. Chem. Soc. 2022, 144, 1106−1112

*430074, People's Republic of China;* orcid.org/0000-0003-4612-2268

**Alex J. Plajer** − *Department of Chemistry, University of Cambridge, Cambridge CB2 1EW, United Kingdom; Oxford Chemistry, Chemical Research Laboratory, Oxford OX1 3TA, U.K.*

**Roy Lavendomme** − *COMOC—Center for Ordered Materials, Organometallics and Catalysis, Department of Chemistry, Ghent University, 9000 Ghent, Belgium;* orcid.org/0000-0001-6238-8491

**Tanya K. Ronson** − *Department of Chemistry, University of Cambridge, Cambridge CB2 1EW, United Kingdom;* orcid.org/0000-0002-6917-3685

**Zifei Lu** − *Department of Chemistry, University of Cambridge, Cambridge CB2 1EW, United Kingdom*

**Jesper D. Jensen** − *Department of Chemistry & Nano-Science Center, University of Copenhagen, 2100 Copenhagen, Denmark*

**Bo W. Laursen** − *Department of Chemistry & Nano-Science Center, University of Copenhagen, 2100 Copenhagen, Denmark;* orcid.org/0000-0002-1120-3191

Complete contact information is available at: https://pubs.acs.org/10.1021/jacs.1c11536

### Notes

The authors declare no competing financial interest.

## ■ ACKNOWLEDGMENTS

This work was supported by the European Research Council (695009) and the UK Engineering and Physical Sciences Research Council (EPSRC EP/P027067/1). The authors thank the Department of Chemistry NMR facility, University of Cambridge, for performing some NMR experiments and Diamond Light Source (UK) for synchrotron beamtime on I19 (CY21497). D.Z. acknowledges a Herchel Smith Research Fellowship from the University of Cambridge. Z.L. thanks the Cambridge Trust and the Chinese Scholarship Council for Ph.D. funding.

## ■ REFERENCES

(1) (a) Burke, B. P.; Grantham, W.; Burke, M. J.; Nichol, G. S.; Roberts, D.; Renard, I.; Hargreaves, R.; Cawthorne, C.; Archibald, S. J.; Lusby, P. J. Visualizing kinetically robust $Co^{III}_4L_6$ assemblies in vivo: SPECT imaging of the encapsulated $[^{99m}Tc]TcO_4^-$ anion. *J. Am. Chem. Soc.* **2018**, *140*, 16877−16881. (b) Ozores, H. L.; Amorin, M.; Granja, J. R. Self-assembling molecular capsules based on $\alpha,\gamma$-cyclic peptides. *J. Am. Chem. Soc.* **2017**, *139*, 776−784. (c) Akine, S.; Miyashita, M.; Nabeshima, T. A closed metallomolecular cage that can open its aperture by disulfide exchange. *Chem.—Eur. J.* **2019**, *25*, 1432−1435. (d) Mohankumar, M.; Holler, M.; Meichsner, E.; Nierengarten, J. F.; Niess, F.; Sauvage, J. P.; Delavaux-Nicot, B.; Leoni, E.; Monti, F.; Malicka, J. M.; Cocchi, M.; Bandini, E.; Armaroli, N. Heteroleptic copper(I) pseudorotaxanes incorporating macrocyclic phenanthroline ligands of different sizes. *J. Am. Chem. Soc.* **2018**, *140*, 2336−2347. (e) Han, Y. F.; Jia, W. G.; Yu, W. B.; Jin, G. X. Stepwise formation of organometallic macrocycles, prisms and boxes from Ir, Rh and Ru-based half-sandwich units. *Chem. Soc. Rev.* **2009**, *38*, 3419−3434. (f) Jiao, J.; Tan, C.; Li, Z.; Liu, Y.; Han, X.; Cui, Y. Design and assembly of chiral coordination cages for asymmetric sequential reactions. *J. Am. Chem. Soc.* **2018**, *140*, 2251−2259. (g) Hou, Y. J.; Wu, K.; Wei, Z. W.; Li, K.; Lu, Y. L.; Zhu, C. Y.; Wang, J. S.; Pan, M.; Jiang, J. J.; Li, G. Q.; Su, C. Y. Design and enantioresolution of homochiral Fe(II)-Pd(II) coordination cages from stereolabile metalloligands: stereochemical stability and enantioselective separation. *J. Am. Chem. Soc.* **2018**, *140*, 18183−18191. (h) Chen, L. J.; Yang, H. B.; Shionoya, M. Chiral metallosupramolecular architectures. *Chem. Soc. Rev.* **2017**, *46*, 2555−2576.

(2) (a) Chan, A. K.; Lam, W. H.; Tanaka, Y.; Wong, K. M.; Yam, V. W. Multiaddressable molecular rectangles with reversible host-guest interactions: modulation of pH-controlled guest release and capture. *Proc. Natl. Acad. Sci. U.S.A.* **2015**, *112*, 690−695. (b) Bloch, W. M.; Abe, Y.; Holstein, J. J.; Wandtke, C. M.; Dittrich, B.; Clever, G. H. Geometric complementarity in assembly and guest recognition of a bent heteroleptic *cis*-$[Pd_2L^A_2L^B_2]$ coordination cage. *J. Am. Chem. Soc.* **2016**, *138*, 13750−13755. (c) Zhang, Z.; Kim, D. S.; Lin, C. Y.; Zhang, H.; Lammer, A. D.; Lynch, V. M.; Popov, I.; Miljanic, O. S.; Anslyn, E. V.; Sessler, J. L. Expanded porphyrin-anion supramolecular assemblies: environmentally responsive sensors for organic solvents and anions. *J. Am. Chem. Soc.* **2015**, *137*, 7769−7774. (d) Custelcean, R.; Bonnesen, P. V.; Duncan, N. C.; Zhang, X.; Watson, L. A.; Van Berkel, G.; Parson, W. B.; Hay, B. P. Urea-functionalized $M_4L_6$ cage receptors: anion-templated self-assembly and selective guest exchange in aqueous solutions. *J. Am. Chem. Soc.* **2012**, *134*, 8525−8534. (e) Samanta, S. K.; Moncelet, D.; Briken, V.; Isaacs, L. Metal−organic polyhedron capped with cucurbit[8]uril delivers doxorubicin to cancer cells. *J. Am. Chem. Soc.* **2016**, *138*, 14488−14496. (f) Bruns, C. J.; Fujita, D.; Hoshino, M.; Sato, S.; Stoddart, J. F.; Fujita, M. Emergent ion-gated binding of cationic host-guest complexes within cationic $M_{12}L_{24}$ molecular flasks. *J. Am. Chem. Soc.* **2014**, *136*, 12027−12034.

(3) (a) You, L.; Berman, J. S.; Anslyn, E. V. Dynamic multi-component covalent assembly for the reversible binding of secondary alcohols and chirality sensing. *Nat. Chem.* **2011**, *3*, 943−948. (b) Albrecht, M.; Isaak, E.; Baumert, M.; Gossen, V.; Raabe, G.; Fröhlich, R. "Induced fit" in chiral recognition: epimerization upon dimerization in the hierarchical self-assembly of helicate-type titanium(IV) complexes. *Angew. Chem., Int. Ed.* **2011**, *50*, 2850−2853.

(4) (a) Zhang, D.; Ronson, T. K.; Zou, Y.-Q.; Nitschke, J. R. Metal−organic cages for molecular separations. *Nat. Rev. Chem.* **2021**, *5*, 168−182. (b) Fuertes-Espinosa, C.; Gomez-Torres, A.; Morales-Martinez, R.; Rodriguez-Fortea, A.; Garcia-Simon, C.; Gandara, F.; Imaz, I.; Juanhuix, J.; Maspoch, D.; Poblet, J. M.; Echegoyen, L.; Ribas, X. Purification of uranium-based endohedral metallofullerenes (EMFs) by selective supramolecular encapsulation and release. *Angew. Chem., Int. Ed.* **2018**, *57*, 11294−11299. (c) Catti, L.; Zhang, Q.; Tiefenbacher, K. Advantages of catalysis in self-assembled molecular capsules. *Chem.—Eur. J.* **2016**, *22*, 9060−9066.

(5) Mal, P.; Breiner, B.; Rissanen, K.; Nitschke, J. R. White phosphorus is air-stable within a self-assembled tetrahedral capsule. *Science* **2009**, *324*, 1697−1699.

(6) (a) Yoshizawa, M.; Tamura, M.; Fujita, M. Diels-alder in aqueous molecular hosts: Unusual regioselectivity and efficient catalysis. *Science* **2006**, *312*, 251−254. (b) Kaphan, D. M.; Levin, M. D.; Bergman, R. G.; Raymond, K. N.; Toste, F. D. A supramolecular microenvironment strategy for transition metal catalysis. *Science* **2015**, *350*, 1235−1238. (c) Omagari, T.; Suzuki, A.; Akita, M.; Yoshizawa, M. Efficient catalytic epoxidation in water by axial N-ligand-free Mn-porphyrins within a micellar capsule. *J. Am. Chem. Soc.* **2016**, *138*, 499−502. (d) Cullen, W.; Misuraca, M. C.; Hunter, C. A.; Williams, N. H.; Ward, M. D. Highly efficient catalysis of the Kemp elimination in the cavity of a cubic coordination cage. *Nat. Chem.* **2016**, *8*, 231−236. (e) Howlader, P.; Das, P.; Zangrando, E.; Mukherjee, P. S. Urea-functionalized self-assembled molecular prism for heterogeneous catalysis in water. *J. Am. Chem. Soc.* **2016**, *138*, 1668−1676. (f) Fang, Y.; Powell, J. A.; Li, E.; Wang, Q.; Perry, Z.; Kirchon, A.; Yang, X.; Xiao, Z.; Zhu, C.; Zhang, L.; Huang, F.; Zhou, H. C. Catalytic reactions within the cavity of coordination cages. *Chem. Soc. Rev.* **2019**, *48*, 4707−4730. (g) Zhao, L.; Jing, X.; Li, X.; Guo, X.; Zeng, L.; He, C.; Duan, C. Catalytic properties of chemical transformation within the confined pockets of Werner-type capsules. *Coord. Chem. Rev.* **2019**, *378*, 151−187. (h) Galli, M.; Lewis, J. E.; Goldup, S. M. A stimuli-responsive rotaxane-gold catalyst:

regulation of activity and diastereoselectivity. *Angew. Chem., Int. Ed.* **2015**, *54*, 13545−13549.
(7) (a) Zhang, D.; Ronson, T. K.; Nitschke, J. R. Functional capsules via subcomponent self-assembly. *Acc. Chem. Res.* **2018**, *51*, 2423−2436. (b) Zhou, X.-P.; Wu, Y.; Li, D. Polyhedral metal-imidazolate cages: control of self-assembly and cage to cage transformation. *J. Am. Chem. Soc.* **2013**, *135*, 16062−16065. (c) Sham, K. C.; Yiu, S. M.; Kwong, H. L. Dodecanuclear hexagonal-prismatic $M_{12}L_{18}$ coordination cages by subcomponent self-assembly. *Inorg. Chem.* **2013**, *52*, 5648−5650. (d) Young, M. C.; Holloway, L. R.; Johnson, A. M.; Hooley, R. J. A supramolecular sorting hat: stereocontrol in metal-ligand self-assembly by complementary hydrogen bonding. *Angew. Chem., Int. Ed.* **2014**, *53*, 9832−9836. (e) Ren, D. H.; Qiu, D.; Pang, C. Y.; Li, Z.; Gu, Z. G. Chiral tetrahedral iron(II) cages: diastereoselective subcomponent self-assembly, structure interconversion and spin-crossover properties. *Chem. Commun.* **2015**, *51*, 788−791. (f) Yi, S.; Brega, V.; Captain, B.; Kaifer, A. E. Sulfate-templated self-assembly of new $M_4L_6$ tetrahedral metal organic cages. *Chem. Commun.* **2012**, *48*, 10295−10297. (g) Domer, J.; Slootweg, J. C.; Hupka, F.; Lammertsma, K.; Hahn, F. E. Subcomponent assembly and transmetalation of dinuclear helicates. *Angew. Chem., Int. Ed.* **2010**, *49*, 6430−6433. (h) Lewing, D.; Koppetz, H.; Hahn, F. E. Reversible formation and transmetalation of schiff-base complexes in subcomponent self-assembly reactions. *Inorg. Chem.* **2015**, *54*, 7653−7659. (i) Frischmann, P. D.; Kunz, V.; Wurthner, F. Bright fluorescence and host-guest sensing with a nanoscale $M_4L_6$ tetrahedron accessed by self-assembly of zinc-imine chelate vertices and perylene bisimide edges. *Angew. Chem., Int. Ed.* **2015**, *54*, 7285−7289. (j) Roukala, J.; Zhu, J.; Giri, C.; Rissanen, K.; Lantto, P.; Telkki, V. V. Encapsulation of xenon by a self-assembled $Fe_4L_6$ metallosupramolecular cage. *J. Am. Chem. Soc.* **2015**, *137*, 2464−2467. (k) Howson, S. E.; Bolhuis, A.; Brabec, V.; Clarkson, G. J.; Malina, J.; Rodger, A.; Scott, P. Optically pure, water-stable metallo-helical 'flexicate' assemblies with antibiotic activity. *Nat. Chem.* **2012**, *4*, 31−36.
(8) (a) Wang, H.; Liu, C. H.; Wang, K.; Wang, M.; Yu, H.; Kandapal, S.; Brzozowski, R.; Xu, B.; Wang, M.; Lu, S.; Hao, X. Q.; Eswara, P.; Nieh, M. P.; Cai, J.; Li, X. Assembling pentatopic terpyridine ligands with three types of coordination moieties into a giant supramolecular hexagonal prism: synthesis, self-assembly, characterization, and antimicrobial study. *J. Am. Chem. Soc.* **2019**, *141*, 16108−16116. (b) Fujita, D.; Ueda, Y.; Sato, S.; Yokoyama, H.; Mizuno, N.; Kumasaka, T.; Fujita, M. Self-assembly of $M_{30}L_{60}$ icosidodecahedron. *Chem.* **2016**, *1*, 91−101. (c) Wang, G.; Chen, M.; Wang, J.; Jiang, Z.; Liu, D.; Lou, D.; Zhao, H.; Li, K.; Li, S.; Wu, T.; Jiang, Z.; Sun, X.; Wang, P. Reinforced topological nanoassemblies: 2D hexagon-fused wheel to 3D prismatic metallo-lamellar structure with molecular weight of 119 K daltons. *J. Am. Chem. Soc.* **2020**, *142*, 7690−7698. (d) Pasquale, S.; Sattin, S.; Escudero-Adán, E. C.; Martínez-Belmonte, M.; de Mendoza, J. Giant regular polyhedra from calixarene carboxylates and uranyl. *Nat. Commun.* **2012**, *3*, 785. (e) Chen, Y. S.; Solel, E.; Huang, Y. F.; Wang, C. L.; Tu, T. H.; Keinan, E.; Chan, Y. T. Chemical mimicry of viral capsid self-assembly via corannulene-based pentatopic tectons. *Nat. Commun.* **2019**, *10*, 3443.
(9) (a) Douglas, T.; Young, M. Host−guest encapsulation of materials by assembled virus protein cages. *Nature* **1998**, *393*, 152−155. (b) Stagg, S. M.; LaPointe, P.; Razvi, A.; Gurkan, C.; Potter, C. S.; Carragher, B.; Balch, W. E. Structural basis for cargo regulation of COPII coat assembly. *Cell* **2008**, *134*, 474−484. (c) Prasad, B. V.; Hardy, M. E.; Dokland, T.; Bella, J.; Rossmann, M. G.; Estes, M. K. X-ray crystallographic structure of the Norwalk virus capsid. *Science* **1999**, *286*, 287−290.
(10) (a) Fujita, D. Challenges to large molecular encapsulation. *Pur. Appl. Chem.* **2014**, *86*, 3−11. (b) Fujita, D.; Suzuki, K.; Sato, S.; Yagi-Utsumi, M.; Yamaguchi, Y.; Mizuno, N.; Kumasaka, T.; Takata, M.; Noda, M.; Uchiyama, S.; Kato, K.; Fujita, M. Protein encapsulation within synthetic molecular hosts. *Nat. Commun.* **2012**, *3*, 1093.
(11) (a) Saibil, H. R.; Fenton, W. A.; Clare, D. K.; Horwich, A. L. Structure and allostery of the chaperonin GroEL. *J. Mol. Biol.* **2013**, *425*, 1476−1487. (b) Nussinov, R. Introduction to protein ensembles and allostery. *Chem. Rev.* **2016**, *116*, 6263−6266.
(12) Wang, W.; Wang, Y. X.; Yang, H. B. Supramolecular transformations within discrete coordination-driven supramolecular architectures. *Chem. Soc. Rev.* **2016**, *45*, 2656−2693.
(13) (a) Kishi, N.; Akita, M.; Kamiya, M.; Hayashi, S.; Hsu, H. F.; Yoshizawa, M. Facile catch and release of fullerenes using a photoresponsive molecular tube. *J. Am. Chem. Soc.* **2013**, *135*, 12976−12979. (b) Dube, H.; Ajami, D.; Rebek, J., Jr. Photochemical control of reversible encapsulation. *Angew. Chem., Int. Ed.* **2010**, *49*, 3192−3195. (c) Han, M.; Michel, R.; He, B.; Chen, Y. S.; Stalke, D.; John, M.; Clever, G. H. Light-triggered guest uptake and release by a photochromic coordination cage. *Angew. Chem., Int. Ed.* **2013**, *52*, 1319−1323. (d) Kim, T. Y.; Vasdev, R. A. S.; Preston, D.; Crowley, J. D. Strategies for reversible guest uptake and release from metallosupramolecular architectures. *Chem.—Eur. J.* **2018**, *24*, 14878−14890. (e) Samanta, S. K.; Quigley, J.; Vinciguerra, B.; Briken, V.; Isaacs, L. Cucurbit[7]uril enables multi-stimuli-responsive release from the self-assembled hydrophobic phase of a metal organic polyhedron. *J. Am. Chem. Soc.* **2017**, *139*, 9066−9074. (f) Wu, H.; Chen, Y.; Zhang, L.; Anamimoghadam, O.; Shen, D.; Liu, Z.; Cai, K.; Pezzato, C.; Stern, C. L.; Liu, Y.; Stoddart, J. F. A dynamic tetracationic macrocycle exhibiting photoswitchable molecular encapsulation. *J. Am. Chem. Soc.* **2019**, *141*, 1280−1289.
(14) Chen, J.; Wezenberg, S. J.; Feringa, B. L. Intramolecular transport of small-molecule cargo in a nanoscale device operated by light. *Chem. Commun.* **2016**, *52*, 6765−6768.
(15) Shanmugaraju, S.; Umadevi, D.; Savyasachi, A. J.; Byrne, K.; Ruether, M.; Schmitt, W.; Watson, G. W.; Gunnlaugsson, T. Reversible adsorption and storage of secondary explosives from water using a Tröger's base-functionalised polymer. *J. Mater. Chem. A* **2017**, *5*, 25014−25024.
(16) (a) Cullen, W.; Turega, S.; Hunter, C. A.; Ward, M. D. pH-dependent binding of guests in the cavity of a polyhedral coordination cage: reversible uptake and release of drug molecules. *Chem. Sci.* **2015**, *6*, 625−631. (b) Mura, S.; Nicolas, J.; Couvreur, P. Stimuli-responsive nanocarriers for drug delivery. *Nat. Mater.* **2013**, *12*, 991−1003. (c) Giglio, V.; Varela-Aramburu, S.; Travaglini, L.; Fiorini, F.; Seeberger, P. H.; Maggini, L.; De Cola, L. Reshaping silica particles: mesoporous nanodiscs for bimodal delivery and improved cellular uptake. *Chem. Eng. J.* **2018**, *340*, 148−154.
(17) (a) Chen, S.; Chen, L. J.; Yang, H. B.; Tian, H.; Zhu, W. Light-triggered reversible supramolecular transformations of multi-bisthienylethene hexagons. *J. Am. Chem. Soc.* **2012**, *134*, 13596−13599. (b) Oldknow, S.; Martir, D. R.; Pritchard, V. E.; Blitz, M. A.; Fishwick, C. W. G.; Zysman-Colman, E.; Hardie, M. J. Structure-switching $M_3L_2$ Ir(III) coordination cages with photo-isomerising azo-aromatic linkers. *Chem. Sci.* **2018**, *9*, 8150−8159. (c) Diaz-Moscoso, A.; Ballester, P. Light-responsive molecular containers. *Chem. Commun.* **2017**, *53*, 4635−4652.
(18) (a) Kishimoto, M.; Kondo, K.; Akita, M.; Yoshizawa, M. A pH-responsive molecular capsule with an acridine shell: catch and release of large hydrophobic compounds. *Chem. Commun.* **2017**, *53*, 1425−1428. (b) Kim, S. H.; Kim, K. R.; Ahn, D. R.; Lee, J. E.; Yang, E. G.; Kim, S. Y. Reversible regulation of enzyme activity by pH-responsive encapsulation in DNA nanocages. *ACS Nano* **2017**, *11*, 9352−9359. (c) Kaizerman-Kane, D.; Hadar, M.; Tal, N.; Dobrovetsky, R.; Zafrani, Y.; Cohen, Y. pH-responsive pillar[6]arene-based water-soluble supramolecular hexagonal boxes. *Angew. Chem., Int. Ed.* **2019**, *58*, 5302−5306.
(19) (a) Wang, S.; Yao, C.; Ni, M.; Xu, Z.; Cheng, M.; Hu, X.-Y.; Shen, Y.-Z.; Lin, C.; Wang, L.; Jia, D. Thermo- and oxidation-responsive supramolecular vesicles constructed from self-assembled pillar[6]arene-ferrocene based amphiphilic supramolecular diblock copolymers. *Polym. Chem.* **2017**, *8*, 682−688. (b) Zhang, D.; Ronson, T. K.; Guryel, S.; Thoburn, J. D.; Wales, D. J.; Nitschke, J. R. Temperature controls guest uptake and release from $Zn_4L_4$ tetrahedra.


https://doi.org/10.1021/jacs.1c11536
J. Am. Chem. Soc. 2022, 144, 1106−1112

*J. Am. Chem. Soc.* **2019**, *141*, 14534−14538. (c) Chan, M. H.; Leung, S. Y.; Yam, V. W. Rational design of multi-stimuli-responsive scaffolds: synthesis of luminescent oligo(ethynylpyridine)-containing alkynylplatinum(II) polypyridine foldamers stabilized by Pt···Pt interactions. *J. Am. Chem. Soc.* **2019**, *141*, 12312−12321.

(20) (a) Heo, J.; Jeon, Y. M.; Mirkin, C. A. Reversible interconversion of homochiral triangular macrocycles and helical coordination polymers. *J. Am. Chem. Soc.* **2007**, *129*, 7712−7713. (b) Baxter, P. N. W.; Khoury, R. G.; Lehn, J.-M.; Baum, G.; Fenske, D. Adaptive self-assembly: environment-induced formation and reversible switching of polynuclear metallocyclophanes. *Chem.—Eur. J.* **2000**, *6*, 4140−4148. (c) Kilbas, B.; Mirtschin, S.; Scopelliti, R.; Severin, K. A solvent-responsive coordination cage. *Chem. Sci.* **2012**, *3*, 701−704. (d) Gidron, O.; Jirasek, M.; Trapp, N.; Ebert, M. O.; Zhang, X.; Diederich, F. Homochiral [2]catenane and bis[2]catenane from alleno-acetylenic helicates - a highly selective narcissistic self-sorting process. *J. Am. Chem. Soc.* **2015**, *137*, 12502−12505.

(21) (a) Frischmann, P. D.; Kunz, V.; Stepanenko, V.; Wurthner, F. Subcomponent self-assembly of a 4 nm $M_4L_6$ tetrahedron with Zn(II) vertices and perylene bisimide dye edges. *Chem.—Eur. J.* **2015**, *21*, 2766−2769. (b) Weilandt, T.; Troff, R. W.; Saxell, H.; Rissanen, K.; Schalley, C. A. Metallo-supramolecular self-assembly: the case of triangle-square equilibria. *Inorg. Chem.* **2008**, *47*, 7588−7598. (c) Lu, X.; Li, X.; Guo, K.; Xie, T. Z.; Moorefield, C. N.; Wesdemiotis, C.; Newkome, G. R. Probing a hidden world of molecular self-assembly: concentration-dependent, three-dimensional supramolecular interconversions. *J. Am. Chem. Soc.* **2014**, *136*, 18149−18155. (d) Yamamoto, T.; Arif, A. M.; Stang, P. J. Dynamic equilibrium of a supramolecular dimeric rhomboid and trimeric hexagon and determination of its thermodynamic constants. *J. Am. Chem. Soc.* **2003**, *125*, 12309−12317.

(22) Zhang, D.; Ronson, T. K.; Xu, L.; Nitschke, J. R. Transformation network culminating in a heteroleptic $Cd_6L_6L'_2$ twisted trigonal prism. *J. Am. Chem. Soc.* **2020**, *142*, 9152−9157.

(23) (a) Li, B.; Zhang, W.; Lu, S.; Zheng, B.; Zhang, D.; Li, A.; Li, X.; Yang, X. J.; Wu, B. Multiple transformations among anion-based $A_{2n}L_{3n}$ assemblies: bicapped trigonal antiprism $A_8L_{12}$, tetrahedron $A_4L_6$, and triple helicate $A_2L_3$ (A = Anion). *J. Am. Chem. Soc.* **2020**, *142*, 21160−21168. (b) Zhang, T.; Zhou, L. P.; Guo, X. Q.; Cai, L. X.; Sun, Q. F. Adaptive self-assembly and induced-fit transformations of anion-binding metal-organic macrocycles. *Nat. Commun.* **2017**, *8*, 15898. (c) Riddell, I. A.; Ronson, T. K.; Clegg, J. K.; Wood, C. S.; Bilbeisi, R. A.; Nitschke, J. R. Cation- and anion-exchanges induce multiple distinct rearrangements within metallosupramolecular architectures. *J. Am. Chem. Soc.* **2014**, *136*, 9491−9498. (d) Cullen, W.; Hunter, C. A.; Ward, M. D. An interconverting family of coordination cages and a meso-helicate; effects of temperature, concentration, and solvent on the product distribution of a self-assembly process. *Inorg. Chem.* **2015**, *54*, 2626−2637.

(24) Plajer, A. J.; Percastegui, E. G.; Santella, M.; Rizzuto, F. J.; Gan, Q.; Laursen, B. W.; Nitschke, J. R. Fluorometric recognition of nucleotides within a water-soluble tetrahedral capsule. *Angew. Chem., Int. Ed.* **2019**, *58*, 4200−4204.

(25) Bilbeisi, R. A.; Ronson, T. K.; Nitschke, J. R. A self-assembled $[Fe^{II}_{12}L_{12}]$ capsule with an icosahedral framework. *Angew. Chem., Int. Ed.* **2013**, *52*, 9027−9030.

(26) Kleywegt, G. J.; Jones, T. A. Detection, delineation, measurement and display of cavities in macromolecular structures. *Acta Crystallogr.* **1994**, *D50*, 178−185.

(27) (a) Rizzuto, F. J.; Nitschke, J. R. Stereochemical plasticity modulates cooperative binding in a $Co^{II}_{12}L_6$ cuboctahedron. *Nat. Chem.* **2017**, *9*, 903−908. (b) Ramsay, W. J.; Szczypinski, F. T.; Weissman, H.; Ronson, T. K.; Smulders, M. M.; Rybtchinski, B.; Nitschke, J. R. Designed enclosure enables guest binding within the 4200 $A^3$ cavity of a self-assembled cube. *Angew. Chem., Int. Ed.* **2015**, *54*, 5636−5640.

(28) (a) Zhang, D.; Ronson, T. K.; Greenfield, J. L.; Brotin, T.; Berthault, P.; Leonce, E.; Zhu, J. L.; Xu, L.; Nitschke, J. R. Enantiopure $[Cs^+/Xe\subset$cryptophane$]\subset Fe^{II}_4L_4$ hierarchical superstructures. *J. Am. Chem. Soc.* **2019**, *141*, 8339−8345. (b) Ronson, T. K.; League, A. B.; Gagliardi, L.; Cramer, C. J.; Nitschke, J. R. Pyrene-edged $Fe^{II}_4L_6$ cages adaptively reconfigure during guest binding. *J. Am. Chem. Soc.* **2014**, *136*, 15615−15624.

(29) Bilbeisi, R. A.; Clegg, J. K.; Elgrishi, N.; de Hatten, X.; Devillard, M.; Breiner, B.; Mal, P.; Nitschke, J. R. Subcomponent self-assembly and guest-binding properties of face-capped $Fe_4L_4^{8+}$ capsules. *J. Am. Chem. Soc.* **2012**, *134*, 5110−5119.

(30) Bai, X.; Jia, C.; Zhao, Y.; Yang, D.; Wang, S. C.; Li, A.; Chan, Y. T.; Wang, Y. Y.; Yang, X. J.; Wu, B. Peripheral templation-modulated interconversion between an $A_4L_6$ tetrahedral anion cage and $A_2L_3$ triple helicate with guest capture/release. *Angew. Chem., Int. Ed.* **2018**, *57*, 1851−1855.

(31) Zhang, D.; Ronson, T. K.; Mosquera, J.; Martinez, A.; Guy, L.; Nitschke, J. R. Anion binding in water drives structural adaptation in an azaphosphatrane-functionalized $Fe^{II}_4L_4$ tetrahedron. *J. Am. Chem. Soc.* **2017**, *139*, 6574−6577.

(32) Percastegui, E. G.; Ronson, T. K.; Nitschke, J. R. Design and applications of water-soluble coordination cages. *Chem. Rev.* **2020**, *120*, 13480−13544.



https://doi.org/10.1021/jacs.1c11536
*J. Am. Chem. Soc.* 2022, 144, 1106−1112